

# Preparation of Toughened PMMA through PEG-Modified Urethane Acrylate/PMMA Core–Shell Composite Particles

JIN-GYU PARK,<sup>1</sup> JU-YOUNG KIM,<sup>2</sup> KYUNG-DO SUH<sup>1</sup>

<sup>1</sup> Department of Industrial Chemistry, College of Engineering, Hanyang University, Seoul 133-791, South Korea

<sup>2</sup> School of Chemical Engineering, Olin Hall, Cornell University, Ithaca, New York 14853-5201

Received 5 February 1997; accepted 17 February 1998

**ABSTRACT:** Poly(urethane acrylate) (PUA)/poly(methylmethacrylate) (PMMA) core–shell composite particles were prepared by two-stage emulsion polymerization. The sizes of composite particles could be varied from 25 to 210 nm by introducing polyoxyethylene (POE) groups to the urethane acrylate molecular backbone. Core–shell morphology was identified by investigating the polarity of the surface of the core and shell polymer particles and by measuring the contact angle of the composite particles. A composite particle prepared with relatively small particles (about 20 nm) did not show the core/shell morphology, because the high polar surface of the core polymer particle and the low-stage ratio of the core to the shell cause the formation of a core/shell two-stage latex to be more thermodynamically unstable. The fracture toughness of rubber-toughened PMMA containing PUA/PMMA composite particles increased as the particle sizes decreased and the shell thickness of the composite particles increased. In particular, when the average size of the composite particle was about 43 nm and the stage ratio was 50/50, the fracture toughness of the rubber-toughened PMMA increased more than three times compared with that of pure PMMA. Furthermore, the transparency of toughened PMMA could be maintained up to 91% in the visible spectra range.  
© 1998 John Wiley & Sons, Inc. *J Appl Polym Sci* 69: 2291–2302, 1998

**Key words:** PEG-modified urethane acrylate; core–shell; composite particle; fracture toughness; transparency

## INTRODUCTION

PMMA resin is commonly used as a surface-coating material as well as a fabrication material. It is also widely used as a housing material or surface-coating material of machinery because of its excellent weather resistance and high transparency. However, the range of application is limited by its inherent brittleness. Thus, studies for improving its toughness and retaining its transparency have been carried out actively.<sup>1,2</sup>

There are two ways to improve the toughness of PMMA: One is to copolymerize methyl methacrylate (MMA) with another monomer that has a low glass transition temperature ( $T_g$ ).<sup>3</sup> The other is to blend it with other rubbery polymers through physical blending or a graft reaction.<sup>4–6</sup> In using composite polymer particles as a toughening agent, core–shell particles comprise two or more radially alternating rubbery- and glassy-layer polymers, the center always being of a rubbery (elastomeric) polymer such as polybutadiene, poly(butyl acrylate), or SBR and the outer layer of the glassy polymer compatible with the matrix polymer.<sup>7–11</sup> When PMMA is blended with the core–shell composite particles, there would be many toughening mechanisms, such as interval

Correspondence to: J.-Y. Kim.

Contract grant sponsor: Engineering Research Center (ERC) for Functional Polymer of Korea.

*Journal of Applied Polymer Science*, Vol. 69, 2291–2302 (1998)

© 1998 John Wiley & Sons, Inc.

CCC 0021-8995/98/112291-12

cavitation of the rubber particles, prior formation of shear bands,<sup>12,13</sup> crack deflection and particle bridging, and rubber particle stretching.

Although the impact strength of PMMA can be improved by using conventional two-stage composite particles based on a rubbery polymer like polybutadiene, poly(butyl acrylate), and SBR, its transparency cannot be maintained because the relatively large particle of conventional composite latex makes PMMA opaque. Thus, it becomes essential to prepare nano-scale composite latex to prepare impact-modified PMMA retaining its original transparency.

The ultimate goal of this study was the preparation of a nano-scale composite particle using poly(ethylene glycol)-modified urethane acrylate (PMUA)<sup>14,15</sup> and the investigation of the effect of particle sizes on the fracture toughness and transparency of PMMA. In our previous article,<sup>15,16</sup> nano-scale polyurethane latex having different droplet sizes could be obtained by the emulsion polymerization of PMUA. We also prepared polyurethane/poly(glycidyl methacrylate)-*co*-acrylonitrile nanocomposite particles having different particle sizes by using this nano-scale polyurethane latex. These particles could improve the impact strength of the epoxy resin more than 20 times compared with that of pure epoxy resin.<sup>16</sup>

Generally, in the case of emulsion polymerization of a conventional monomer, it is difficult to control the size of the emulsion droplets. Although the droplet size of this emulsion can be changed by the amount and kind of surfactant used and the mixing method, there is a limit in the control of the droplet size; moreover, an excess amount of surfactant should be used to prepare nano-scale particles, which can exert a bad effect on the property of the final product. However, PMUA latex has nano-scale particles, and its droplet size could be controlled by the number of terminal polyoxyethylene (POE) groups, because the hydrophilicity of PMUA changed largely with the number of these hydrophilic groups.<sup>14,15</sup>

The morphology of the composite particle strongly depends on the particle surface polarity and the size of the first-stage particle (core polymer).<sup>17–20</sup> Thus, four kinds of PUA latexes are prepared by using four kinds of PMUA having different hydrophilicity to investigate the effect of the core particle size and stage ratio on the morphology of poly(urethane acrylate) (PUA)/poly(methyl methacrylate) (PMMA) composite particles. In addition, 12 kinds of composite particles will be prepared by using those four kinds

**Table I Molar Ratio of Each Reagent for the Synthesis of PMUA**

	PTMG	TDI	2-HEMA	PEG600
PMUA1	1	2	1.85	0.15
PMUA2	1	2	1.7	0.3
PMUA3	1	2	1.5	0.5
PMUA4	1	2	1.2	0.8

of PUA latex and used as a impact-modifier for PMMA.

## EXPERIMENTAL

### Reagents

In the synthesis of poly(ethylene glycol)-modified urethane acrylate (PMUA), poly(tetramethylene glycol) (PTMG, MW = 1000, Hyosung BASF, Korea), 2,4-toluene diisocyanate (TDI, Junsei Chemical Co., Japan), 2-hydroxyethyl methacrylate (2-HEMA, Aldrich Chemical Co., Milwaukee, WI), and poly(ethylene glycol) (PEG, MW = 600, Junsei Chemical Co.) were used. Inhibitors of methyl methacrylate monomer (MMA) and tetramethylene glycol dimethacrylate (TEGDMA, Aldrich Chemical Co.), used as crosslinking agents, were removed through a removing column (Aldrich Chemical Co.). 2,2'-Azobisisobutyronitrile (AIBN), an oil-soluble initiator, was recrystallized by absolute methanol and dried at 30°C in a decompressed condition for 3 days. Sodium lauryl sulfate (SLS, Aldrich Chemical Co.) was also used as an emulsifier.

### Synthesis of PMUA<sup>14,15</sup>

All PMUA samples were synthesized by three-step processes. The molar ratios of the reactants are summarized in Table I and the molecular structure of PMUA is illustrated in Figure 1. These reactions were carried out in a four-necked glass reactor equipped with a stirrer, thermometer, reflux condenser, and inlet system for N<sub>2</sub> gas. A detailed reaction mechanism was also reported in our previous articles.<sup>14,15</sup>

According to our previous experimental results, in the case where the molecular weight of PEG was 600, PMUA showed the smallest droplet size and the highest emulsion stability.

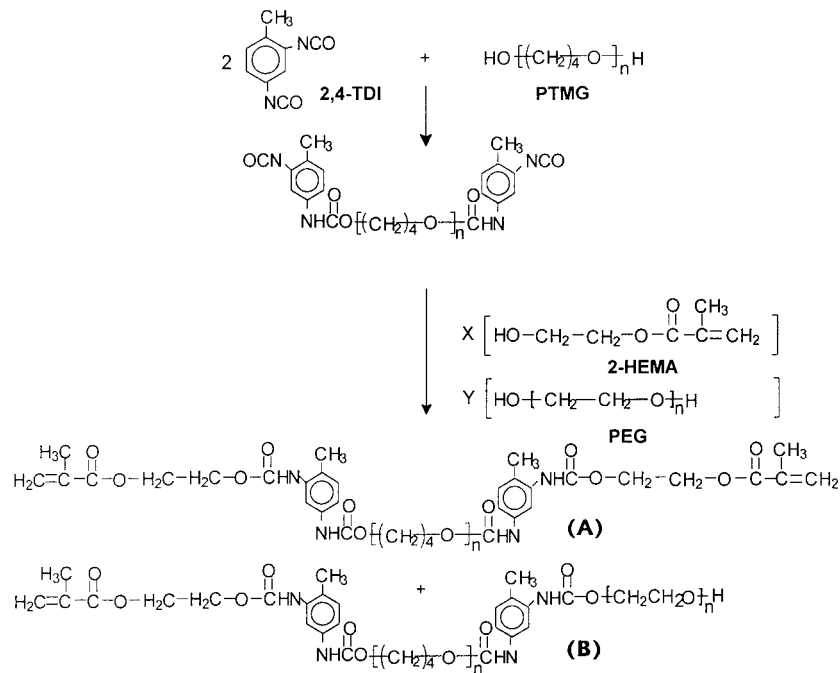


**Figure 1** Molecular structure of PMAU.

### Preparation of Core-Shell Composite Particles

In the case of the preparation of PMUA emulsions, the mixture of the modified urethane acrylate (10 g), AIBN (0.02 g), and SLS (0.01 g) were charged in a glass reactor equipped with stirrer, thermocouples, and reflux condenser, and then distilled deionized water (DDI water) was dropped into the reactor at the rate of 0.375 g/min at room temperature. When the preparation of the PMUA emulsion was completed, the reactor was heated to the initiation temperature of AIBN, 55°C. When the polymerization was carried out for 6 h, the conversion rate was about 98%. The recipe for the emulsion polymerization of PMUA is summarized in Table II.

In the second stage of the emulsion polymerization, that is, the addition of MMA and TEGDMA monomers, the shell formation was performed

through a semibatch process in which the monomers containing AIBN (1 wt %) were added continuously into the reactor from a microdropping funnel at the constant rate of 0.04 g/min. The shell polymerization was carried out at 55°C for 6 h while the agitation speed was 160 rpm. The recipe for the preparation of PUA/PMMA latex is summarized in Table III. The sample notation used for the PUA/PMMA composite particles is CPUM $x$ - $y/z$ , where  $x$  is the kind of PUA core polymer and  $y/z$  is the stage ratio (weight ratio) of the core to the shell. For example, CPUM4-50/50 is a PUA/PMMA composite particle prepared using the PUA4 core particle at a 50/50 stage ratio of core/shell.

The average sizes of the composite particles were measured by a laser light scattering instrument (Brook Heaven Co. Ltd., BI9000AT, argon laser). To obtain powders of the composite parti-

**Table II** Recipe for the Emulsion Polymerization of PMUA and the Size of PMUA Latex Formed by Emulsion Polymerization

Symbol	PMUA	DDI Water (g)	AIBN (g)	SLS (g)	Particle Size (nm)
PUA1	PMUA1 10 g	90	0.2	0.1	175.24
PUA2	PMUA2 10 g	90	0.2	0.1	86.67
PUA3	PMUA3 10 g	90	0.2	0.1	44.33
PUA4	PMUA4 10 g	90	0.2	0.1	22.40

**Table III** Recipe for the Preparation of PUA/PMMA Composite Latex and Its Particle Size

Symbols	PUA Latex <sup>a</sup>	MMA (g)	DDI Water (g)	AIBN (g)	Particle Size (nm)
CPUM1-70/30	PUA1 100 g	4.290	30	0.042	184.20
CPUM1-60/40	PUA1 100 g	6.670	30	0.067	198.40
CPUM1-50/50	PUA1 100 g	10.00	30	0.100	209.56
CPUM1-70/30	PUA1 100 g	4.290	30	0.042	93.00
CPUM1-60/40	PUA1 100 g	6.670	30	0.067	114.33
CPUM1-50/50	PUA1 100 g	10.00	30	0.100	130.33
CPUM1-70/30	PUA1 100 g	4.290	30	0.042	51.00
CPUM1-60/40	PUA1 100 g	6.670	30	0.067	57.00
CPUM1-50/50	PUA1 100 g	10.00	30	0.100	67.67
CPUM1-70/30	PUA1 100 g	4.290	30	0.042	24.33
CPUM1-60/40	PUA1 100 g	6.670	30	0.067	37.00
CPUM1-50/50	PUA1 100 g	10.00	30	0.100	43.00

<sup>a</sup> PUA latex contains 10 g of polymerized PMUA and 90 g of DDI water. Thus, in the case when 4.290 g of MMA is added at the second emulsion polymerization, the stage ratio, meaning the weight ratio, of PUA/PMMA is 70/30.

cles, prepared core-shell latexes were deemulsified with CaCl<sub>2</sub> and filtered. Then, they were dried at 50°C for 48 h. These composite particles were used as a fracture toughness modifier of PMMA.

### Contact-angle Measurement

To obtain a solid surface free from impurities, which are likely to influence its surface properties, all latex samples were dried in a vacuum oven at 50°C. DDI water and methylene iodide (CH<sub>2</sub>I<sub>2</sub>; 1 μL) were dropped on each sample film, and the contact angle was determined by a contact angle meter (Erma contact angle meter, Model G-1). With these observed contact angles of DDI water and CH<sub>2</sub>I<sub>2</sub>, the surface tension ( $\gamma_s$ ), surface polarity ( $\gamma_s^p$ ), and surface dispersity ( $\gamma_s^d$ ) were calculated by the geometric-mean method.<sup>16</sup> All measurements are the average of 10 runs. The surface tension ( $\gamma_s$ ) was calculated by the Owens' equation<sup>21</sup>:

$$\gamma_s = \gamma_s^p + \gamma_s^d \quad (1)$$

where  $\gamma_s$  is the summation of the polar component ( $\gamma_s^p$ ) and dispersity component ( $\gamma_s^d$ ). Although there have been some differences between the harmonic-mean and geometric-mean method, the latter was chosen because it was possible to infer the morphology of the composite particle with only relative surface polarities. Daniels et al. suggested that the surface of the core polymer

particle has an effect on the morphology of a two-stage composite latex.<sup>22</sup> Therefore, the morphology of the composite particles could be identified by using the surface polarity of the core polymer (PUA). Also, the effect of the surface polarity of the core polymer particle on the morphology also could be investigated.

### Sample Preparation

To prepare sheets that are used in the measurement of the toughness of toughened PMMA, AIBN and the composite particles were mixed with the MMA monomer. Then, this mixture was poured into a glass frame mold sealed with silicon rubber. This mold was immersed in the water bath and polymerized at 40°C for 24 h. After this process, postcuring was carried out at 80°C for 5 h. All specimens contained 10 wt % of the toughening particles.

### Scanning Electron Microscopy and Transmission Electron Microscopy

A scanning electron microscope (SEM: Philips Co. XL-30) was used to investigate the dispersity of the particles in the PMMA matrix. The cross section of the samples was analyzed by the conventional secondary electron imaging technique. Samples were coated with a thin layer of gold-palladium to reduce any charge buildup on the fracture surface.

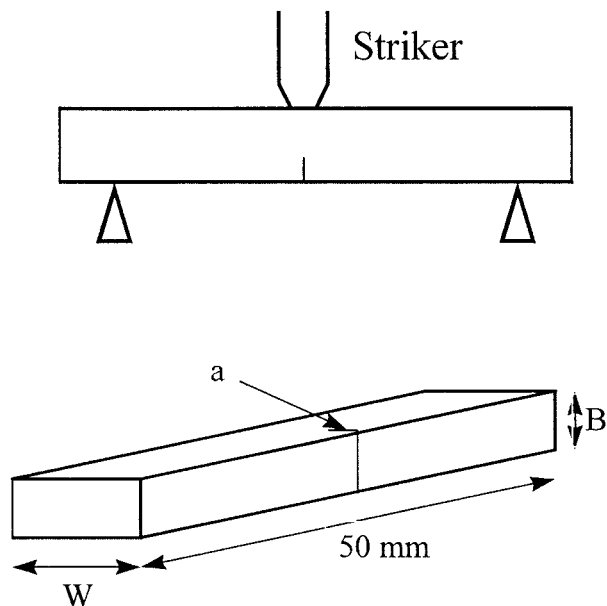


**Figure 2** Three-point bending testing method and the geometry of the testing specimen.

The dispersion of the composite particle in the PMMA matrix was observed by transmission electron microscopy (TEM, Hitachi HU11-E). Ultra-thin samples were obtained by microtoming molded specimens using a Riechert-Jung ultramicrotome at  $-80^{\circ}\text{C}$ . Staining was carried out by using  $\text{OsO}_4$  (1% solution in water) for at least 24 h and/or  $\text{RuO}_4$  (vapor) for a maximum of 15 min.

**Measurement**

The single-edge notched three-point-bend (SENB) specimens were prepared by cutting the toughened PMMA sheets.<sup>16</sup> The geometry of specimen is illustrated in Figure 2.

The fracture toughness and deflection at break of the SENB specimen were measured with a Housefield Model Instron equipped with a three-point-bending tester at room temperature. All measurements are the average of 10 runs. The value of the fracture toughness or stress intensity factor,  $K_{1c}$ , at the onset of crack growth may be deduced from the measured force,  $F_c$ , at crack initiation by the following equation<sup>23</sup>:

$$K_{1c} = (6F_c Y a^{1/2})(BW) \quad (2)$$

where  $a$  is the length of a sharp crack;  $B$ , the thickness;  $W$ , the width of the specimen; and  $Y$ , a dimensionless geometry factor which is given by

$$Y = \frac{(1.99 - \{a/W(1 - a/W)\} \times [2.15 - 3.93a/W + 2.7(a/W)^2])}{(1 + 2a/W)(1 - a/W)^{1.5}} \quad (3)$$

Transparency was measured by using a UV-visible spectrophotometer (Shimadzu UV-2010PC). The transparencies of the 3-mm-thick sheets were compared by measuring the transmission of rays at a 500-nm wavelength.

**RESULTS AND DISCUSSION**

**Preparation of PUA Core Latex**

The PUA/PMMA core-shell composite latex could be prepared by two-stage emulsion polymerization. A semibatch process was employed to minimize the formation of new particles during the second-stage polymerization and to be more favorable of forming the core-shell morphology thermodynamically. At the first emulsion polymerization, PMUA was soap-free emulsified and polymerized to be used as a core particle of the composite particles. The size of the core particles could be controlled in the range of 22–175 nm. The size of the core particle is summarized in Table II.

The formation of nano-scale PUA particles is due to the interfacial activity of molecules containing POE groups. In other words, PMUA molecules containing POE groups act as a polymeric surfactant, so that PMUA emulsions can make a fine and stable dispersion in water with a relatively small amount of surfactant.<sup>14,15,24</sup> Thus, the size of the PUA particle can be controlled by the number of POE groups. As the molar ratio of PEG to 2-HEMA increased in the synthesis of PMUA, the size of the PUA particles decreases almost regularly because of the increase in the number of molecules having terminal POE groups (Table II). The distribution of the particle size of PMUA latex is represented in Figure 3.

**Preparation of PUA/PMMA Composite Latex**

At the first emulsion polymerization, as previously mentioned, nano-scale core particles were prepared by the emulsion polymerization of PMUA. As the second stage, the second emulsion polymerization of MMA was carried out by a semi-batch process. The MMA monomer was added into the PUA emulsion and polymerized at  $55^{\circ}\text{C}$  for 6 h. It was assumed that PMMA surrounds PUA

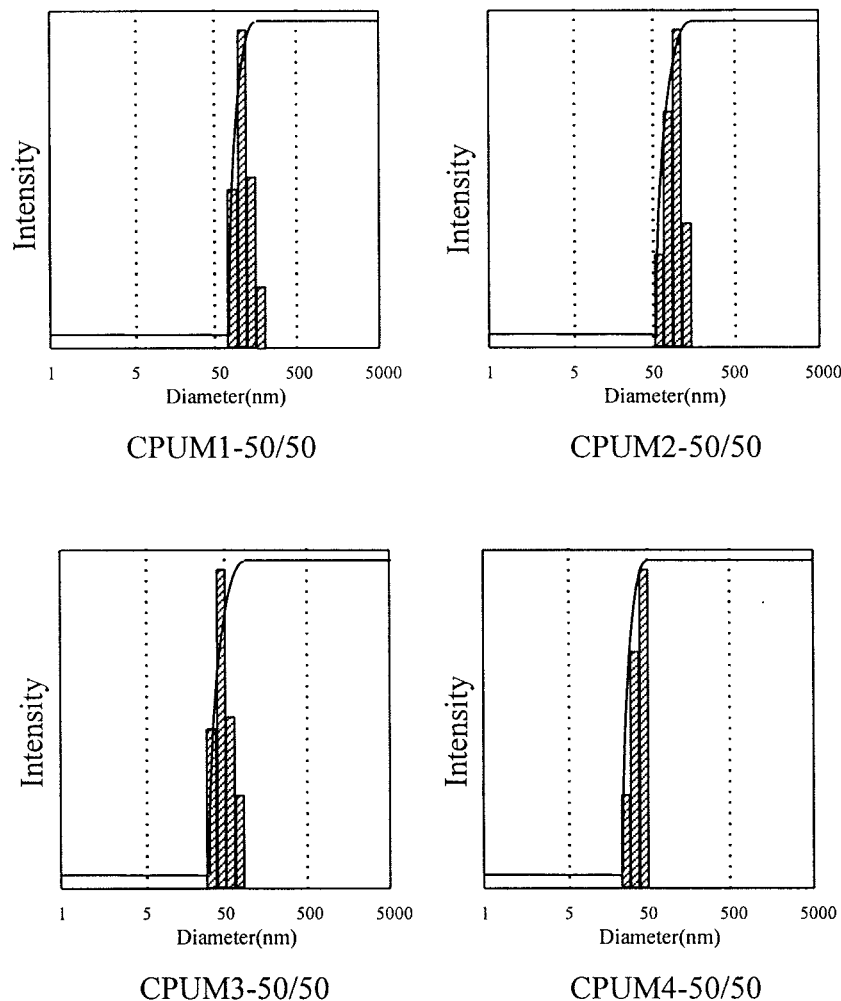


**Figure 3** Particle-size distributions of PUA core latexes. Laser light scattering was used to obtain average particle sizes and their distribution: (A) PUA1 core latex; (B) PUA2 core latex; (C) PUA3 core latex; (D) PUA4 core latex.

particles in the course of the second emulsion polymerization and forms the shell of composite particles. The weight ratio of the MAA to PUA particles (stage ratio) was varied to investigate the effect of the added amount of MAA on the formation of composite particles.

If the shell of the composite particles formed by the polymerization of MMA is not crosslinked, the linear PMMA shell polymer could dissolve in the MMA monomer during the preparation of the toughened PMMA sheets. In other words, in the case where the morphology of the composite particles cannot be maintained in the course of mixing the composite particles with the MMA monomer, phase separation between the PMMA matrix and the urethane core polymer in the PMMA matrix occurred. Thus, the shell was crosslinked by TEG-

DMA (0.01 g) to retain its morphology in the course of the preparation of the PMMA sheets. Figure 4 shows the particle-size distributions of the PUA/PMMA composite latexes.

The sizes of the composite particles are narrow and fine ones, and the particle size also increases as the stage ratio of MMA to PUA particles increases, that is, as the added amount of MMA increases (Table III). Finally, the sizes of the composite particles could be controlled from 25 to 209 nm (Table III).

#### Identification of Core–Shell Morphology Through Surface Polarity

To use PUA/PMMA composite particles as a toughening agent for PMMA, these particles

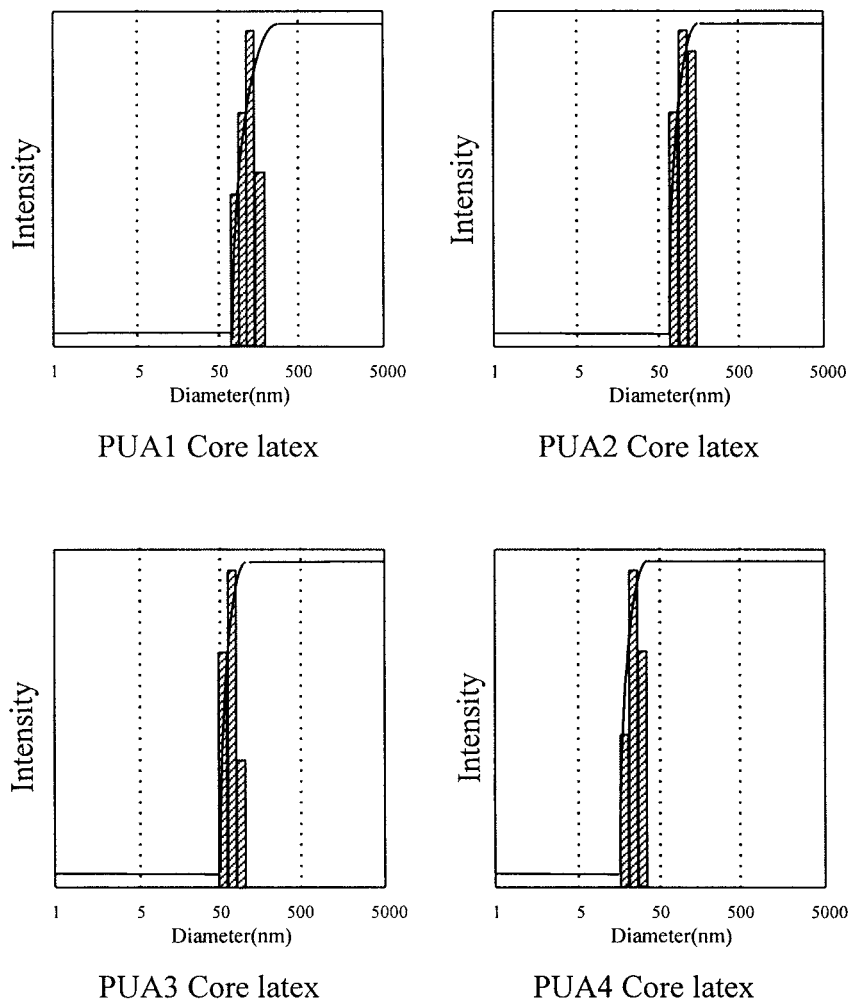


**Figure 4** Particle-size distributions of PUA/PMMA core-shell latexes: (A) CPUM1-50/50; (B) CPUM2-50/50; (C) CPUM3-50/50; (D) CPUM4-50/50.

should have a core-shell morphology, that is, the outer layer is crosslinked PMMA and the inner layer is PUA. The PUA is inherently incompatible with PMMA, so those PUA particles should be coated with PMMA to increase their dispersibility and to form nano-scale dispersed PUA domains at the PMMA matrix. Therefore, it can be thought that the morphology of the composite particles is a decisive factor for the rubber-toughening PMMA; thus, the identification of the composite particle morphology should be carried out prior to the application of these composite particles for toughening agents. In our study, contact angle measurement was used to identify the core-shell morphology.

When DDI water as a polar-component and methylene iodide (CH<sub>2</sub>I<sub>2</sub>) as a nonpolar compo-

nent are located on the polymer surface, the contact angle ( $\theta$ ) can be determined by the polymer surface properties, such as surface polarity and surface dispersity. If the core/shell morphology were formed, the surface characteristics of the shell polymer should be the same as those of the shell polymer latex only (in our study, the PMMA latex), because the core particles should be completely surrounded by the shell polymer in the case of the core/shell composite particles. In addition, the surface characteristics of the core can be also examined by the contact angle. The surface polarity with the core particle is one of factors influencing the formation of the core-shell morphology.<sup>22,25-27</sup>

In the PUA/PMMA system, we can consider three thermodynamics factors: surface polarity,

**Table IV Surface Polarity of Latex Film (PMUA and Composite Latex)**

Sample	$\gamma_s$	$\gamma_s^d$	$\gamma_s^p$
PUA1	42.50	35.20	7.30
CPUM1-70/30	49.27	36.48	12.79
CPUM1-60/40	50.42	37.13	13.29
CPMU1-50/50	49.92	37.36	12.56
PUA2	47.85	37.35	10.50
CPUM2-70/30	49.36	36.81	12.55
CPUM2-60/40	50.72	37.28	13.45
CPUM2-50/50	49.87	37.18	12.69
PUA3	53.40	34.39	19.01
CPUM3-70/30	50.71	37.42	13.29
CPUM3-60/40	50.29	37.30	12.99
CPUM3-50/50	49.46	37.02	12.45
PUA4	54.95	33.65	21.30
CPUM4-70/30	51.59	37.36	14.24
CPUM4-60/40	50.01	37.08	12.93
CPUM4-50/50	49.67	36.97	12.70
PMMA	49.13	37.03	12.01

Unit: dyne/cm.

core-shell stage ratio, and core particle size. We could obtain the surface polarity ( $\gamma_s^p$ ) using contact angles of DDI water and  $\text{CH}_2\text{I}_2$  through the Owens' equation. Table IV shows the surface polarities of the polymer films. The surface polarity of the PMUA polymer increases, as the molar ratio of PEG to 2-HEMA in the regular sequence (Table I). This is because the hydrophilicity of PUA increases with the number of molecules having POE groups in PMUA.

The surface polarities of the composite particle films show similarities to those of the PMMA film (12.45–12.93 dyne/cm). This result could be confirmed by the formation of the PUA/PMMA core/shell morphology. However, for the CPUM4-70/30 core-shell latex, the surface polarity is 14.24 dyne/cm, much higher than that of the PMMA film, indicating that the core/shell morphology is not formed. The PUA4 core particle has a considerably higher surface polarity (21.30 dyne/cm) than PMMA (12.10 dyne/cm) and any other PUA particles. It is suggested that the hydrophobe-water surface formed by PMMA would be replaced by a hydrophile-water surface made of PMUA4, causing the formation of the inverted or mixed morphology to be more favorable.

It has been reported that the formation of the core/shell morphology becomes thermodynamically

unfavorable with increase of the hydrophilicity of the core particles.<sup>22,28</sup> For example, in the case of the PMMA/polystyrene (PS) (hydrophilic/hydrophobic) system, the formation of the inverted core/shell morphology is the most thermodynamically favorable arrangement. This is because the interfacial tension between PS and water is greater than the PMMA–water interfacial tension. In other words, the formation of an inverted morphology eliminates the most unfavorable hydrophobic-water surface and replaces it with a hydrophilic-water surface.<sup>22,27,28</sup> Therefore, as the number of molecules having a POE group in PMUA, the size of the core particles decreases, whereas the formation of the core/shell morphology becomes unfavorable because of the increase in the hydrophilicity of the core polymer.

Moreover, it has also been reported that the stage ratio or weight ratio of the core/shell polymer influences the morphology of the composite particles,<sup>25–27</sup> that is, as the relative amounts of the second polymer or shell polymer increases, the core/shell morphology becomes more favorable. Thus, in the case of CPUM4-70/30, the weight ratio of the second polymer (MMA) to the core polymer is the smallest and the hydrophilicity of the core polymer (PUA) is greater than that of any other core polymer, so the formation of the core/shell morphology is most unfavorable among the PUA/PMMA composite particles.

### Fracture Toughness Tendencies

In our experiment, core-shell composite particles were used as a toughening agent of PMMA. To investigate the optimum particle size for toughening PMMA, we varied the size of composite particles in the region of 25–210 nm, where a good shear band formation was expected with the same materials, PEG-modified urethane acrylate, and MMA.<sup>9,16,29–31</sup> Core-shell composite particles also have advantages in the aspect that they can maintain the spherical morphology of the rubber particles and that it is possible for them to form a significantly small rubber particle domain to about 23 nm. Therefore, the affection of small composite particles on the PMMA toughness could be investigated according to the particle sizes of the core-shell composite particles.

The three-point bending test was used to estimate the fracture toughness of the PMMA resin blended with the composite particles.<sup>16</sup> In this experiment, the force at break was measured and the fracture toughness was calculated by eq. (2).



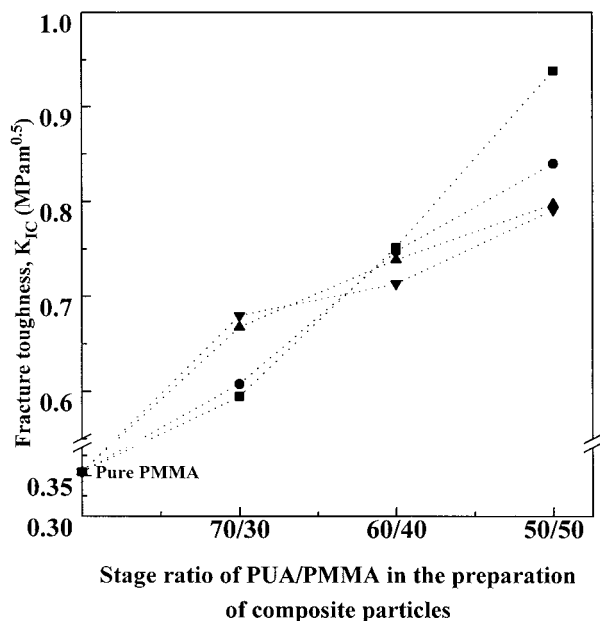


**Figure 5** Change of fracture toughness of toughened PMMA containing PUA/PMMA with the stage ratio of core/shell. The content of the core-shell composite particles is 10 wt % for the PMMA resin: (— ■ —) CPUM4; (— ● —) CPUM3; (— ▲ —) CPUM2; (— ▼ —) CPUM1.

Figure 5 shows the change of the fracture toughness with the stage ratio of the core/shell.

All the specimens contain 10 wt % of the composite particles. PMMA samples blended with CPUM4 particles show the greatest fracture toughness among the CPUM particles. This result is probably due to the smallest size of the CPUM4 particles among the PUA/PMMA composite particles, because the formation of the shear band is more favorable when smaller composite particles are mixed. Although CPUM4-70/30 is the smallest particle among the CPUM4 particles, the PMMA sample mixed with CPUM4-70/30 shows the lowest fracture toughness, because this particle does not have a core/shell morphology. On the other hand, when the PUA/PMMA particles prepared with a 70/30-stage ratio, such as CPUM1-70/30, CPUM2-70/30, CPUM3-70/30, and CPUM4-70/30, are blended with PMMA, CPUM1-70/30 having the largest particle size showed the greatest fracture toughness among these particles, because of the perfect core/shell morphology of this particle. CPUM4-50/50 has the perfect core/shell morphology, smallest core particle, and thicker shell, so that the PMMA specimen containing this particle shows the great-

est fracture toughness among the CPUM particles.

Figure 6 shows the deflection degree at the breakpoint of each specimen. For the same reason, the CPUM4-50/50 particle exhibits better flexibility than that of any other core series at any stage ratio. This implies that small particles compatible with the matrix can form a shear band easier than can the larger ones.

### Transparency Tendencies

Transparencies of all the specimens were measured by UV-visible spectroscopy. Figure 7 shows the change of transparency with increase of the stage ratio of the core-shell particles. When the CPUM4-50/50 particles are blended with PMMA, the transparency of the specimen shows 91% transmittance. Although CPUM4-70/30 has the smallest particle among the PUA/PMMA particles, PMMA containing this particle did not show good transparency. It seemed to be due to the imperfect formation of the core/shell morphology. This may induce the aggregation of particles in the PMMA matrix during preparation of the specimen.

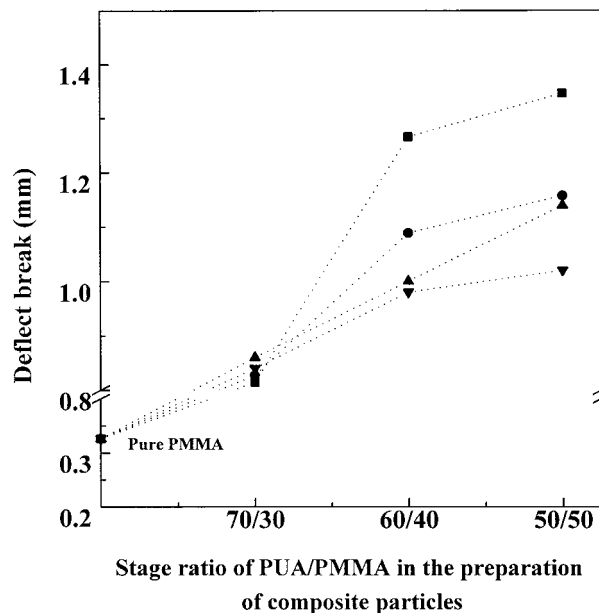


**Figure 6** Change of deflection at break of toughened PMMA containing PUA/PMMA composite particles with the stage ratio of core/shell: (— ■ —) CPUM4; (— ● —) CPUM3; (— ▲ —) CPUM2; (— ▼ —) CPUM1.

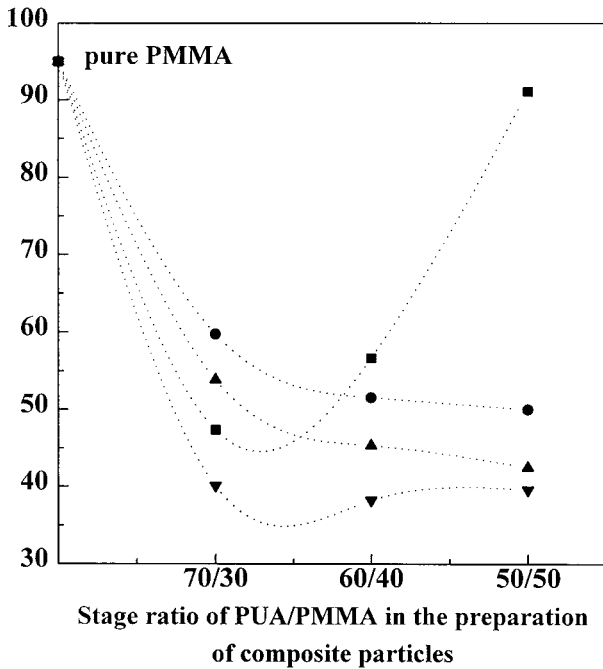


**Figure 7** Change of transparency of toughened PMMA with the stage ratio of shell to core polymer in the synthesis of the composite particles: (— ■ —) blended with CPUM1 series; (— ● —) blended with CPUM2 series; (— ▲ —) blended with CPUM3 series; (— ▼ —) blended with CPUM4 series.

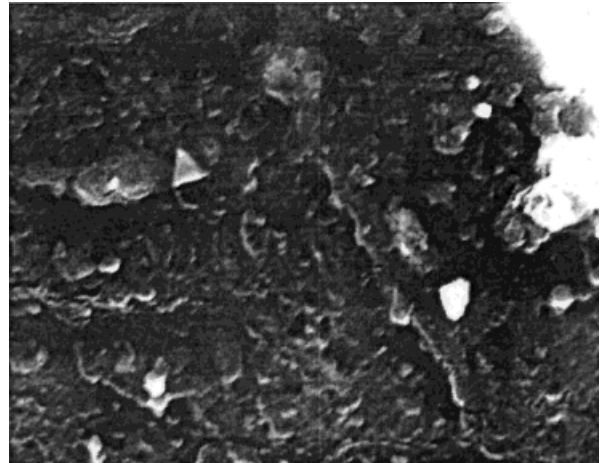
#### Investigation of Dispersity by SEM Images

Figure 8 is an SEM view of the morphology of the PUA/PMMA composite particles (CPUM4-70/30 and CPUM4-50/50) in the PMMA matrix. In the case where the weight ratio of PMUA4/PMMA is 70/30 (CPUM4-70/30), as mentioned above, the possibility of the formation of the core/shell morphology is lower than that of any other composite particle. Therefore, as shown in Figure 6(A), even though the PMMA shell polymer is crosslinked, the coagulum composite particles formed by the aggregation of particles, that is, the core polymer, can be seen in the PMMA matrix. It can be suggested that the low fracture toughness of this specimen is due to the coagulum of the PUA/PMMA particles in the PMMA matrix. In the case of CPUM4-50/50, however, although the same core polymer was used, a thicker shell made it possible to form a perfect dispersed state, as illustrated in Figure 8(B).

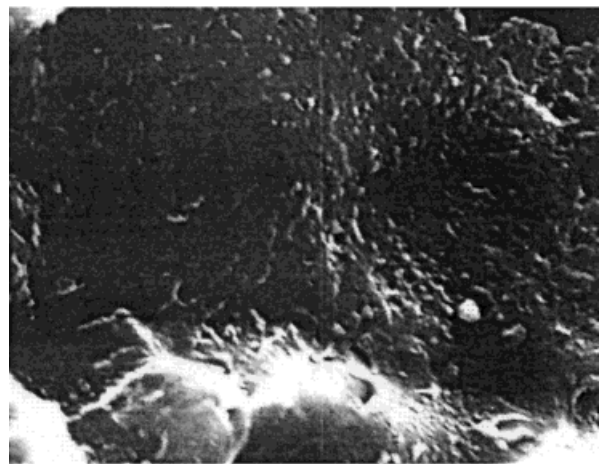
The CPUM4-50/50 particle, the smallest core particle, showed the highest fracture toughness and transparency of any of the PUA/PMMA parti-

cles. This is due to the fine dispersion of the CPUM4-50/50 composite particle at the PMMA matrix. Figure 9 shows the TEM micromorphology of toughened PMMA exhibiting the nano-scale dispersion of the PUA/PMMA composite particle (CPUM4-50/50).

If the PUA/PMMA particles did not have a core/shell morphology, the PUA core particle should be aggregated and form coagulum at the PMMA matrix because of the inherent incompatibility between PUA and PMMA. However, the



A.



B.

**Figure 8** Scanning electron microphotographs of the fractured surface of toughened PMMA: (A) CPUM4-70/30; (B) CPUM4-50/50.

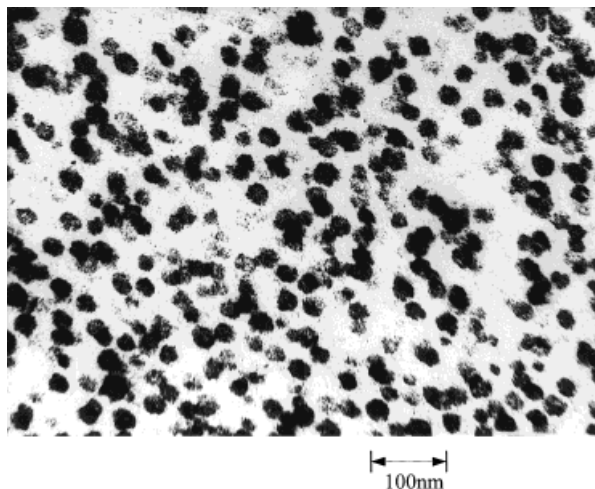


**Figure 9** Transmission electron microphotographs of PMMA matrix containing 10 wt % of PUA/PMMA composite particles (CPUM4-50/50).

TEM microphotograph shows that the PUA core particle is homogeneously dispersed without any aggregation at the PMMA matrix. Therefore, the formation of the core/shell morphology and the homogeneous dispersion of CPUM4-50/50 could be confirmed by the TEM and SEM microphotographs.

## CONCLUSIONS

Four kinds of PUA core particles having different particle sizes could be prepared by using PMUA. As the surface polarity of the core particle increased, the size of the PUA core particle was reduced. Thus, PUA/PMMA composite particles could be prepared in the range of 24–207 nm. As the size of the PUA particles increases, and the stage ratio of the shell to the core increases, the formation of a core/shell morphology becomes favorable.

The fracture toughness of the PMMA resin increased as the shell thickness and size of the composite particles decreased. When the PMUA4 was used as a core polymer at the 50/50 stage ratio of the core/shell (CPUM4-50/50), the fracture toughness was improved more than three times compared with that of the pure PMMA resin. In addition, this specimen containing CPUM4-50/50 exhibited 91% transmittance and the smaller particles showed better fracture toughness, except for the case of the inversion effect of the core-shell morphology. From this result, it could be assumed

that as the composite particle sizes were reduced the dissipation of energy through shear banding was more favorable.

This work was supported by the Engineering Research Center (ERC) for Functional Polymer of Korea.

## REFERENCES

1. K. J. Saunders, *Organic Polymer Chemistry*, Champion & Hall, New York, 1988, p. 62.
2. H. F. Mark, *Encyclopedia of Polymer Science and Engineering*, Vol. 1, Wiley-Interscience, New York, 1985, p. 374.
3. Eur. Patent Pat. 90,109,999 (1990).
4. O. Frank and J. Lehmann, *Colloids Polym. Sci.*, **264**, 473 (1986).
5. C. B. Bucknell, *Toughened Plastics*, Material Science Series, Applied Science, London, 1977.
6. C. B. Bucknell, I. K. Partridge, and M. V. Word, *J. Mater. Sci.*, **19**, 2064 (1984).
7. M. S. Silverstein and M. Narkis, *J. Appl. Polym. Sci.*, **40**, 1583 (1990).
8. M. S. Silverstein and M. Narkis, *J. Appl. Polym. Sci.*, **33**, 2529 (1987).
9. C. K. Riew and A. J. Kinloch, *Toughened Plastics I: Science and Engineering*. Advances in Chemistry Series 233, developed from a symposium sponsored by Division of Polymer Materials Science and Engineering at the 20th National Meeting of the American Chemistry Society, Washington, DC, 1993.
10. D. E. Henton, D. M. Pickelman, C. B. Arends, and V. E. Meyer, U.S. Patent, 4,778,851 (1988).
11. S. Wu, *Polymer Interface and Adhesion*, Marcel Dekker, New York, 1982.
12. W. D. Bascom, R. Y. Ting, and R. J. Moulton, *J. Mater. Sci.*, **16**, 2657 (1981).
13. W. D. Bascom, R. Y. Cottingham, R. L. Jones, and P. Peyser, *J. Appl. Polym. Sci.*, **19**, 2545 (1975).
14. J. Y. Kim and K. D. Suh, *Makromol. Chem.*, **197**, 2429 (1996).
15. J. Y. Kim, and K. D. Suh, *Colloids Polym. Sci.*, **274**, 1025 (1996).
16. J. W. Kim, J. Y. Kim, and K. D. Suh, *J. Appl. Polym. Sci.*, **63**, 1589 (1996).
17. M. Devon, J. Gardon, G. Roberts, and A. Rudin, *J. Appl. Polym. Sci.*, **39**, 2119 (1990).
18. M. Okubo, *Makromol. Chem. Macromol. Symp.*, **35/36**, 307 (1990).
19. D. I. Lee and T. Ishikawa, *J. Polym. Sci. Polym. Chem. Ed.*, **21**, 147 (1983).
20. Y.-C. Chen, M. S. El-Aasser, and V. Dimonie, *J. Appl. Polym. Sci.*, **42**, 1049 (1991).
21. D. K. Owens and R. C. Wendi, *J. Polym. Sci.*, **13**, 1741 (1969).
22. E. S. Daniels, E. D. Sudol, and M. S. El-Aasser, *Polymer Latexes*, ACS Symposium Series 492, de-

- veloped from a symposium sponsored by Division of Polymeric Materials: Science and Engineering at the 21st National Meeting of the American Chemistry Society, Atlanta, GA, April 14–19, 1991.
23. A. J. Kinloch, G. A. Kodokian, and M. B. Jamarani, *J. Mater. Sci.*, **22**, 4111 (1987).
  24. J. Y. Kim and K. D. Suh, *Colloids Polym. Sci.*, **274**, 920 (1996).
  25. J. Berg, D. Sundberg, and B. Kronberg, *J. Microencapsul.*, **6**, 327 (1989).
  26. D. Sundberg, A. P. Casassa, J. Pantazopoulos, M. R. Muscato, B. Kronberg, and J. Berg, *J. Appl. Polym. Sci.*, **45**, 1425 (1990).
  27. J. Berg, D. Sundberg, and B. Kronberg, *Polym. Mater. Sci. Eng.*, **54**, 367 (1983).
  28. I. Cho and K. W. Lee, *J. Appl. Polym. Sci.*, **30**, 1903 (1985).
  29. R. A. Pearson and A. F. Yee, *J. Mater. Sci.*, **26**, 3823 (1991).
  30. J. N. Sulton and F. J. McGarry, *J. Polym. Eng. Sci.*, **13**, 29 (1973).
  31. E. H. Rowe and C. K. Riew, *Plast. Eng., Mar.*, 45 (1975).